JOC The Journal of Organic Chemistry

ARTICLE

pubs.acs.org/joc

# Bis(methylthio)tetracenes: Synthesis, Crystal-Packing Structures, and OFET Properties

Takakazu Kimoto,[†] Kenro Tanaka,[†] Masatoshi Kawahata,[‡] Kentaro Yamaguchi,[‡] Saika Otsubo,[§] Yoshimasa Sakai,[§] Yuuki Ono,[§] Akira Ohno,[§] and Kenji Kobayashi*[,†]

[†]Department of Chemistry, Faculty of Science, Shizuoka University, 836 Ohya, Suruga-ku, Shizuoka 422-8529, Japan,

[‡]Faculty of Pharmaceutical Sciences at Kagawa Campus, Tokushima Bunri University, Shido, Sanuki, Kagawa 769-2193, Japan, and

[§]Mitsubishi Chemical Group Science and Technology Research Center, Inc., 1000 Kamoshida, Aoba-ku, Yokohama 227-8502, Japan

Supporting Information

**ABSTRACT:** 5,12-Bis(methylthio)tetracene (**2**) and 5,11-bis(methylthio)-tetracene (**3**) were synthesized. DFT calculations indicate that the HOMO and LUMO energy levels of **2** and **3** are lowered by 0.13−0.24 eV and their HOMO−LUMO energy gaps are reduced by 0.1 eV relative to those of tetracene. X-ray crystallographic data revealed that **2** is arranged as a result of a 1-D slipped-cofacial $\pi$-stacking with S−S and S−$\pi$ interactions, similar to the packing arrangement of 6,13-bis-(methylthio)pentacene (**1**), whereas **3** exhibits a herringbone packing arrangement without S−S interactions. The OFET devices fabricated using spin-coated films of soluble **1** and **2**, with a bottom-contact device configuration, exhibited hole mobilities as high as $1.3 \times 10^{-2}$ and $4.0 \times 10^{-2}$ cm$^2$ V$^{-1}$ s$^{-1}$ with current on/off ratios of over $10^5$ and $10^4$, respectively.

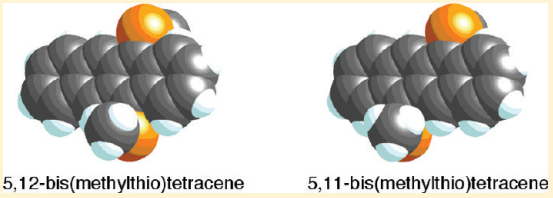


## INTRODUCTION

Acenes, which are made up of linearly annelated benzene rings, and their derivatives are promising candidates as p-type semiconductors for use in organic field-effect transistors (OFETs).[1] Devices based on highly pure single crystals of pentacene and rubrene (5,6,11,12-tetraphenyltetracene) have demonstrated very high field-effect hole mobilities.[2,3] Vacuum-deposited thin film transistors of pentacene also exhibit values up to 3 cm$^2$ V$^{-1}$ s$^{-1}$.[4] However, pentacene is unstable in air and/or light and is subject to oxidation and photooxidation.[1] Pentacene is also almost insoluble in common organic solvents, which makes the use of pentacene difficult as a solution-processable semiconductor.[1] Acenes tend to be susceptible to herringbone packing arrangements with minimal $\pi$-stacking;[5] however, the herringbone-packed pentacene still holds the highest hole mobility among organic semiconductors.[1,2] In general, good electronic performance requires strong electronic coupling between adjacent molecules in the solid state.[6] Realization of a 1-D or 2-D cofacial $\pi$-stacked packing arrangement of acenes might achieve greater charge-carrier transport efficiency because this molecular ordering would facilitate good overlap of the intermolecular $\pi$-orbitals.[1c−e,6b−6f] Rubrene single crystal presents a 2-D herringbone packing in the *ab* plane, but a 1-D largely slipped-cofacial $\pi$-stacking to form tetracene columns along the *a* axis, wherein tetracene rings are slipped relative to each other along the long molecular axis by 6.13 Å, but not slipped along the short molecular axis.[3a,6f] Consequently, mobility in rubrene single crystal is highest along the molecular $\pi$-stacking axis and lowest perpendicular to this axis (edge-to-face direction) and also the cofacial $\pi$-stacking leads to significant overlap of areas of high HOMO density with extrema in the evolution of the transfer integrals upon sliding.[1d,3a,6f]

Thus, improvements in solubility, photooxidative resistance, and control of molecular orientation and arrangement of acenes are very important properties for the development of OFETs.[1,6,7] To resolve these problems associated with acenes, Anthony and co-workers have reported the introduction of bulky trialkylsilylethynyl groups into acenes at appropriate positions.[1,8] It is believed that herringbone packing arrangements of polycyclic aromatic hydrocarbons could be prevented by increasing the ratio of $\pi$-faced carbon atoms to $\pi$-edged hydrogen atoms.[5a,b] Recently, we have demonstrated that S−S and S−$\pi$ interactions assist a cofacial $\pi$-stacking of 9,10-bis(methylthio)anthracene (**4**)[9] and 6,13-bis(methylthio)pentacene (**1**).[10,11] It is noted that the introduction of a small methylthio group into pentacene at the 6,13-positions changes the packing structure from a herringbone to a cofacial $\pi$-stacking motif[10a] and also produces considerable improvements in solubility as well as photooxidative resistance compared with pentacene.[10a,12] Miller and co-workers have reported that arylthio groups are effective to stabilize more unstable larger acenes.[12b,c] The present work is mainly concerned with (1) if S−S and S−$\pi$ interactions generally induce cofacial $\pi$-stacking of bis(methylthio)acenes and (2) the OFET properties of bis(methylthio)acenes as a solution-processable semiconductor. We report here on the synthesis, chemical

**Received:** April 3, 2011
**Published:** May 16, 2011

**Chart 1. Structures of 6,13-Bis(methylthio)pentacene (1), 5,12-Bis(methylthio)tetracene (2), 5,11-Bis(methylthio)-tetracene (3), and 9,10-Bis(methylthio)anthracene (4)**

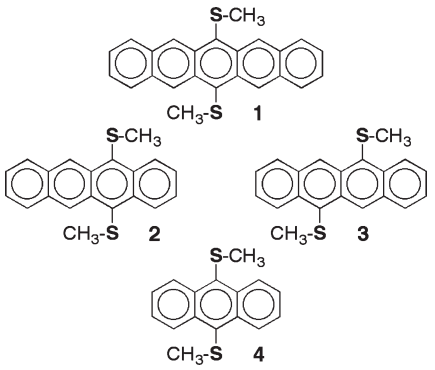


**Scheme 1. Synthesis of (a) 2 and (b) 3**

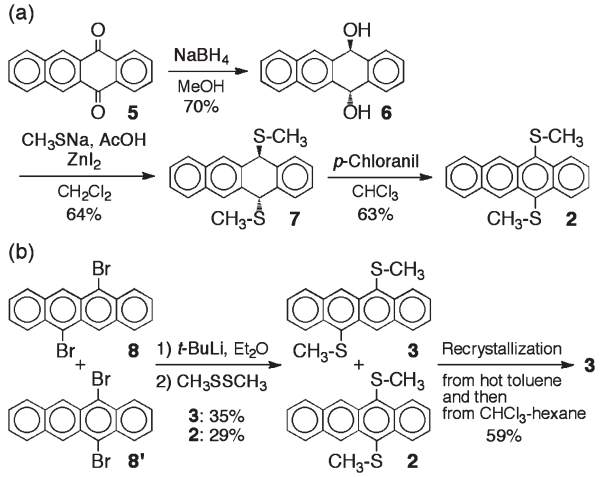


properties, and crystal-packing structures of 5,12-bis(methylthio)-tetracene (**2**) and 5,11-bis(methylthio)tetracene (**3**) (Chart 1)[13−15] and also describe the OFET properties of spin-coated films of **1**−**3** with a bottom-contact device configuration.

## RESULTS AND DISCUSSION

**Synthesis.** 5,12-Bis(methylthio)tetracene (**2**) was synthesized following a three-step procedure similar to that for the synthesis of 6,13-bis(methylthio)pentacene (**1**).[10a] The reduction of 5,12-tetracenequinone (**5**) was carried out with $NaBH_4$, followed by the $ZnI_2$-mediated reaction of *trans*-5,12-dihydroxy-5,12-dihydrotetracene (**6**) with $CH_3SH$,[10a,16] and finally the dehydrogenative aromatization of the resulting *trans*-5,12-bis-(methylthio)-5,12-dihydrotetracene (**7**) with *p*-chloranil to give **2** (Scheme 1a).[17] 5,11-Bis(methylthio)tetracene (**3**) was synthesized by the dilithiation of a mixture of 5,11- and 5,12-dibromotetracenes (**8** and **8′**) with *tert*-butyllithium,[15c] followed by the reaction of 5,11- and 5,12-dilithiotetracenes with dimethyl disulfide. Finally, the resulting mixture of **2** and **3** was repeatedly recrystallized from toluene and then $CHCl_3$−hexane to give pure **3** (Scheme 1b).[17]

**Scheme 2. Photochemical Reactions of (a) 2, (b) 3, and (c) 1 in Both Room Light and Air**

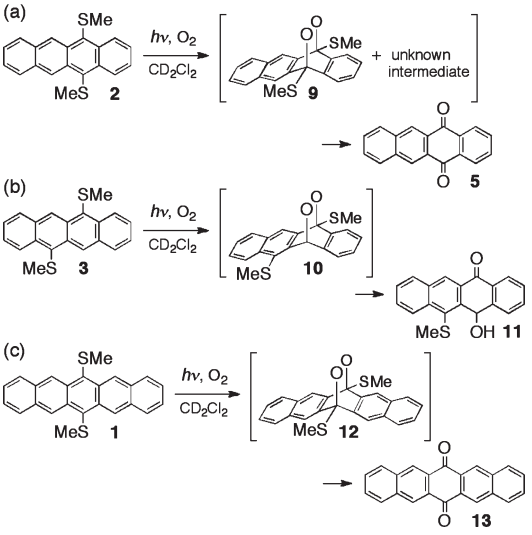


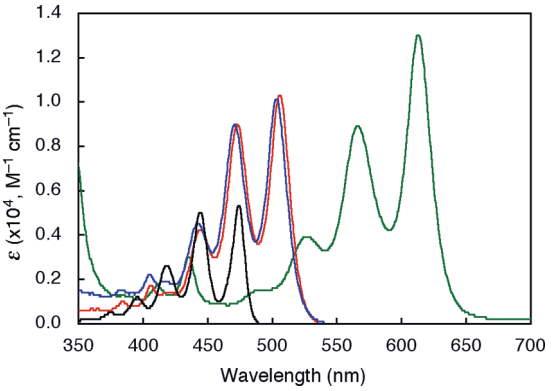


**Figure 1.** UV−vis spectra of **1** (green line), **2** (red line), **3** (blue line), and tetracene (black line) in $CH_2Cl_2$.

**Solubility and Stability.** Bis(methylthio)tetracenes **2** and **3** are soluble in common organic solvents such as $CHCl_3$, THF, and toluene (solubility = >20 mM in $CD_2Cl_2$). Compounds **2** and **3** are stable in air in the absence of light both in solution and in the solid state. However, in both air and room light (fluorescent light), **2** (2 mM) in $CD_2Cl_2$ changed to a mixture of endoperoxide **9** and unknown intermediate after 1.5 h by photooxidation (the half-life of **2** = ca. 30 min), which predominantly decomposed to **5** and dimethyl disulfide after 10 h of photoirradiation (Scheme 2a and Figure S5, Supporting Information).[17] In both air and room light, **3** (2 mM) in $CD_2Cl_2$ almost disappeared after 1 h (the half-life of **3** = ca. 15 min) and changed to a mixture of endoperoxide **10** and semiquinone **11** (Scheme 2b and Figure S6, Supporting Information).[17] After 3 h of photoirradiation, **10** was fully converted to **11**. Surprisingly, the pentacene derivative **1** was more resistant to photooxidation than **2** and **3**,[12a] although it is not easy to elucidate the reason at this stage.[18] In both air and room light, **1** (saturating concentration = 0.8 mM) in $CD_2Cl_2$ showed a half-life of ca. 3 h and predominantly decomposed to 6,13-pentacenequinone (**13**) via


dx.doi.org/10.1021/jo200696a |J. Org. Chem. 2011, 76, 5018–5025

**Table 1. Electrochemical and Optical Properties and HOMO−LUMO Data of 1, 2, 3, and Tetracene**

| compd | 1 | 2 | 3 | tetracene |
|---|---|---|---|---|
| $E_{ox}^{onset}$ (V)[a] | 0.39 | 0.56 | 0.47 | 0.41[c] |
| $E_{red}^{onset}$ (V)[a] | −1.63 | −1.88 | −1.89 | −2.05[c] |
| $E_g^{Echem}$ (eV)[b] | 2.02 | 2.44 | 2.36 | 2.46[c] |
| $\lambda_{max}$ (nm)[d] | 613, 566, 527 | 506, 473, 444 | 503, 471, 442 | 474, 444, 419 |
| log $\varepsilon$ | 4.11, 3.95, 3.59 | 4.01, 3.95, 3.62 | 4.00, 3.95, 3.65 | 3.72, 3.70, 3.41 |
| $\lambda_{cutoff}$ (nm)[e] | 647 | 528 | 528 | 486 |
| $E_g^{Optical}$ (eV)[f] | 1.92 | 2.35 | 2.35 | 2.55 |
| $E_{LUMO}^{DFT}$ (eV)[g] | −2.96 | −2.69 | −2.68 | −2.45 |
| $E_{HOMO}^{DFT}$ (eV)[g] | −5.05 | −5.33 | −5.33 | −5.20 |
| $E_g^{DFT}$ (eV)[h] | 2.09 | 2.64 | 2.65 | 2.75 |

[a] Calculated from the onset of cyclic voltammograms measured in 0.1 M solution of $n$-$Bu_4NClO_4$ as supporting electrolyte in $CH_2Cl_2$, with a Pt electrode and ferrocene as the internal standard. [b] Electrochemical HOMO−LUMO gap. [c] See ref 15d performed in 0.1 M solution of $n$-$Bu_4NPF_6$ in $CH_2Cl_2$. [d] Low energy absorption maxima measured in $CH_2Cl_2$. [e] Wavelength at which the transmittance is 95%. [f] Optical HOMO−LUMO gap based on $\lambda_{cutoff}$. [g] Calculated at B3LYP/6-311+G(d,p)//B3LYP/6-31G(d). [h] Calculated HOMO−LUMO gap.

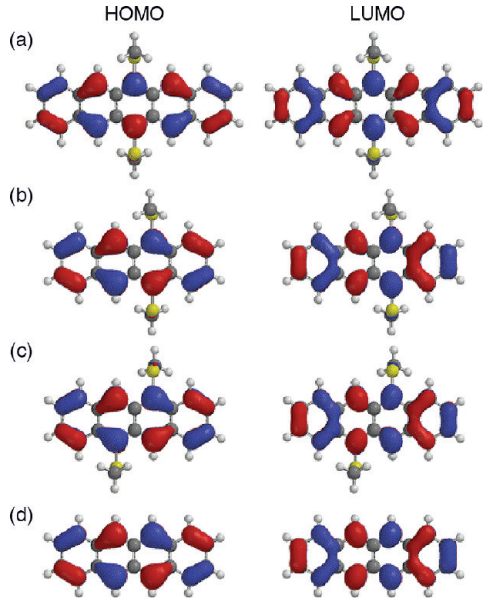


**Figure 2.** HOMO−LUMO diagrams of (a) **1**, (b) **2**, (c) **3**, and (d) tetracene at the B3LYP/6-311+G(d,p)//B3LYP/6-31G(d) level.

endoperoxide **12** after 6 h (Scheme 2c and Figure S8, Supporting Information).[17]

The thermogravimetric differential thermal analyzer (TG-DTA) analysis showed that the melting points of **2** and **3** are 184 and 256 °C, respectively, and at higher temperatures than melting points **2** and **3** begin to decompose with sublimation (Figure S10, Supporting Information).[17] Compound **1** thermally decomposed at 297 °C (Figure S10, Supporting Information).[17] Thus, the thermal stability increased in the order **2** < **3** < **1**.

**Optical and Electrochemical Properties and HOMO−LUMO Calculations.** The UV−vis spectra and spectral data of **2** and **3** in $CH_2Cl_2$ are shown in Figure 1 and Table 1, respectively, as well as compound **1** and tetracene. The longest wavelength absorption maxima ($\lambda_{max}$) for **2** and **3** appeared at 506 and 503 nm, respectively, which were blue-shifted by 107 and 110 nm, respectively, relative to $\lambda_{max}$ of **1** because of shortening of the $\pi$-conjugated acene rings. In contrast, $\lambda_{max}$ for **2** and **3** were red-shifted by 32 and 29 nm, respectively, relative to $\lambda_{max}$ of tetracene because of the reduced HOMO−LUMO gaps induced by the methylthio groups.[9a,10a,12a] The magnitudes of the molar extinction coefficients of $\lambda_{max}$ for **2** and **3** are approximately twice that of tetracene. The reduced HOMO−LUMO gaps of tetracene induced by the introduction of methylthio groups were supported by experimental data

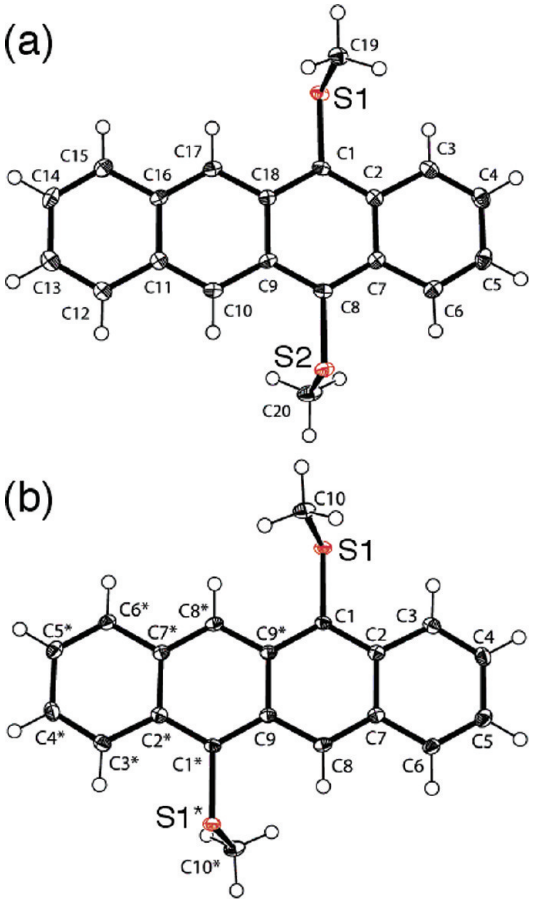


**Figure 3.** ORTEP views of (a) **2** and (b) **3** (50% probability thermal ellipsoids).


dx.doi.org/10.1021/jo200696a |J. Org. Chem. 2011, 76, 5018–5025

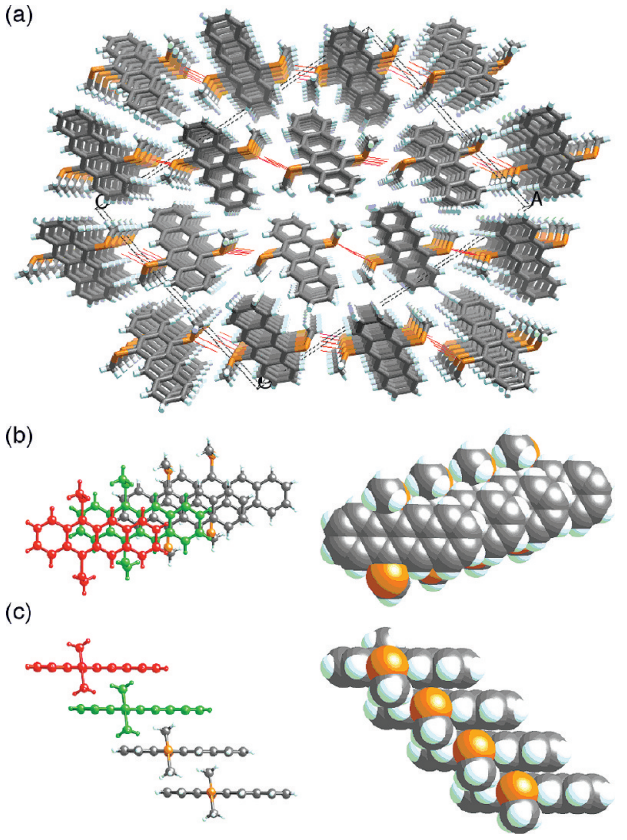


**Figure 4.** (a) 3-D packing structure of **2** in the crystal: perspective view looking down the *b* axis, wherein black and red dotted lines indicate the unit cell and the S−S interactions, respectively. One cofacial $\pi$-stacked column of **2**: (b) top and (c) side views.

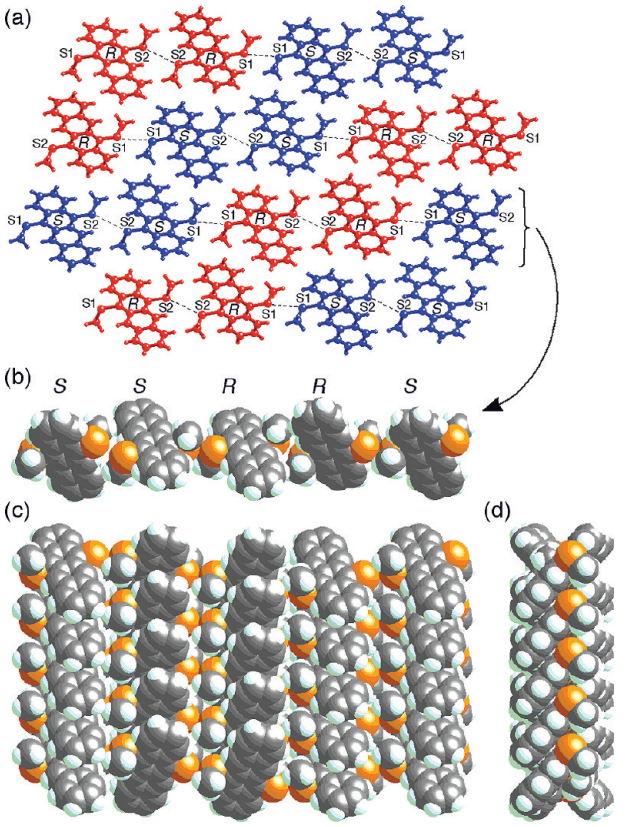


**Figure 5.** (a) 3-D packing diagram viewed down the *b* axis (the same as Figure 4a), wherein *R* and *S* mean the (*R*)-enantiomer (red color) and (*S*)-enantiomer (blue color) of **2** in the crystal. The S1 and S2 show the sulfur atoms, and dotted lines indicate the S−S interactions. One 2-D network sheet of **2** from (a): (b) top view along the *b* axis, (c) front view, and (d) side view.

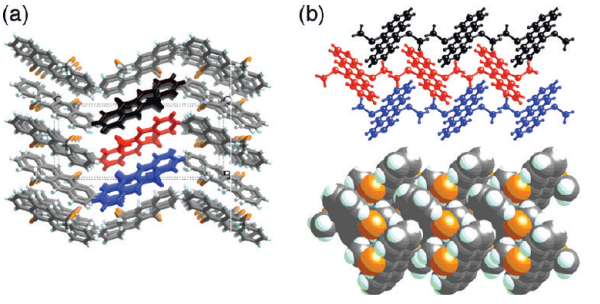


**Figure 6.** 3-D packing structure of **3** in the crystal viewed down (a) the *a* axis and (b) the *c* axis.

obtained with cyclic voltammetry (CV, Figure S11, Supporting Information)[17] and also DFT calculations (B3LYP/6-311+G(d, p)//B3LYP/6-31G(d) level)[12a] of **2** and **3** (Table 1). The introduction of methylthio groups into tetracene lowers both the HOMO and LUMO energy levels by 0.13−0.24 eV relative to those of tetracene. This suggests that **2** and **3** are more susceptible to reduction and less susceptible to oxidation than tetracene. In particular, the lowering of the LUMO energy levels is noticeable. DFT calculations of **2** and **3** also showed that neither the HOMO nor the LUMO are delocalized between the tetracene ring and the sulfur atoms of the methylthio groups (Figure 2). This result suggests that the lowering of both the HOMO and LUMO energy levels, as well as the reduced HOMO−LUMO gaps, of **2** and **3** relative to those of tetracene may be attributed to the electron-withdrawing inductive effect of the methylthio groups[12a] rather than an extension of the $\pi$-conjugation through the methylthio groups.

**X-ray Crystal Structures.** Single crystals of **2** and **3** suitable for X-ray diffraction analysis were obtained by slow diffusion of hexane into a solution of **2** in THF or by slow cooling to room temperature of a hot solution of **3** in $CHCl_3$−hexane. Figure 3 shows the ORTEP views of **2** and **3**, wherein **2** does not have a center of symmetry and **3** has a center of symmetry.

The X-ray crystal packing structure of **2** reveals that **2** is arranged by cofacial $\pi$-stacking along the *b* axis with S−S and S−$\pi$ interactions (Figures 4 and 5).[9a,10a] The tetracene ring of **2** forms the tetracene column through a slipped-cofacial $\pi$-stacking motif along the *b* axis with a face-to-face tetracene−tetracene distance of 3.39 Å. The tetracene rings in one column are slipped relative to each other along the long molecular axis by 3.54 Å and along the short molecular axis by 1.07 Å (Figure 4b,c). These slipped distances are slightly shorter than those of the pentacene derivative **1** (3.64 and 1.19 Å).[10a] The presence of such molecular ordering would permit good overlap of the intermolecular $\pi$-orbitals of the tetracene rings of **2**.[6] There is no S−S interaction (5.078 Å) in the tetracene column. Instead, there are weak intermolecular S−$\pi$ interactions between the sulfur atoms and the neighboring tetracene rings in the tetracene column, with interatomic distances of S1···C3′ = 3.566 Å, S1···C4′ = 3.546 Å,


dx.doi.org/10.1021/jo200696a |*J. Org. Chem.* 2011, 76, 5018–5025

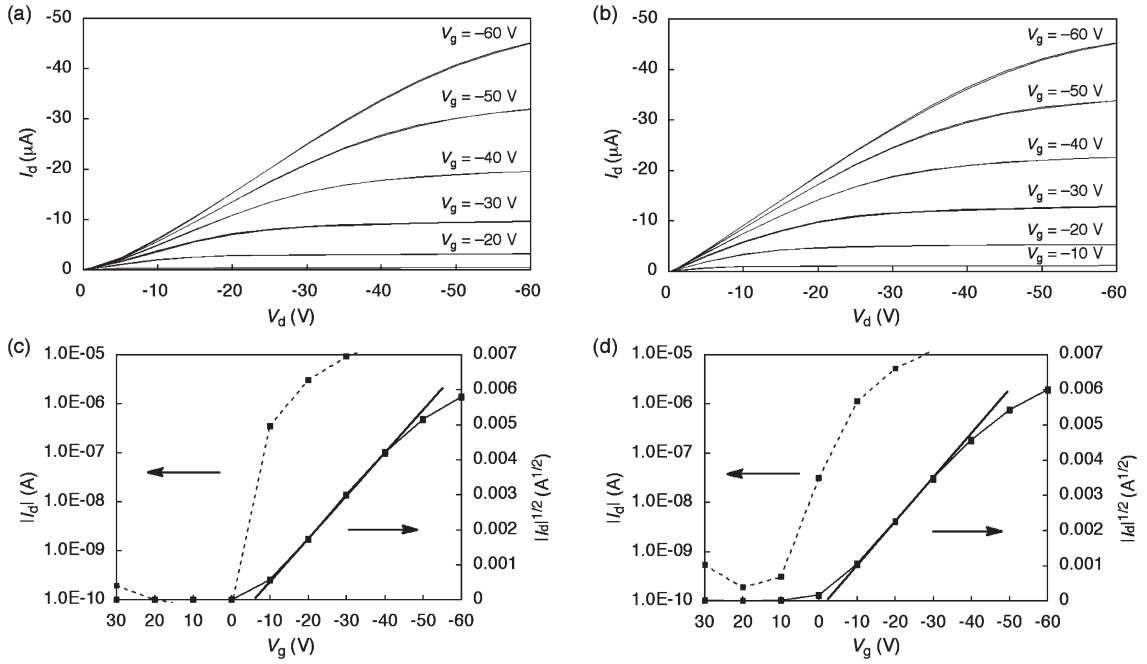


**Figure 7.** *I*−*V* characteristics of bottom-contact FET devices using spin-coated **1** and **2** as the semiconductor layer: output curves at different gate voltages for (a) **1** and (b) **2**; transfer curve in saturated regime at constant source−drain voltage of −40 V and square root of the absolute value of the drain current as a function of gate voltage for (c) **1** and (d) **2**.

S2′···C10 = 3.519 Å, and S2′···C11 = 3.532 Å.[19] They are also somewhat shorter than those determined in **1**, which are ≥3.610 Å for all of these interatomic distances. The S−S interactions exist between the neighboring tetracene columns in **2**, given the interatomic distances of S1···S1′ = 3.370 and S2···S2′ = 3.733 Å (Figures 4a and 5).[19] Thus, self-assembly of bis(methylthio)acenes into 1-D slipped-cofacial π-stacked columns by the assistance of S−S and S−π interactions is proved to be a general phenomenon.[9a,10a] The intermolecular S···S distance of bis(methylthio)acenes decreases in the following order: pentacene **1** (4.297 Å)[10a] > anthracene **4** (3.638 Å)[9a] ≥ tetracene **2** (3.370 and 3.733 Å). These values are still in the range of n−σ* and van der Waals interactions between sulfur atoms.[11,20]

As the molecular symmetry of **2** (Figure 3a) is different from that of **1** and **4**, which both possess a center of symmetry, the 2-D packing arrangement of 1-D cofacial π-stacked columns in **2** is somewhat different from those in **1** and **4** (Figure 5),[9a,10a] although they are all similar in the sense that acene columns formed by slipped-cofacial π-stacking and S−π interactions are linked by S−S interactions to self-assemble into a 2-D network sheet. The crystal form of **2** is found to be racemic as it exists as a 1:1 mixture of (*R*)- and (*S*)-enantiomers. As shown in Figure 5a, each tetracene column of **2** consists of either an (*R*)- or (*S*)-enantiomer, wherein the (*R*)- and (*S*)-columns are shown in red and blue colors, respectively. As shown in Figure 5b−d, the two adjacent parallel tetracene columns are racemic ((*R*)···(*S*)) and are connected by S1···S1′ interactions, whereas the two adjacent staggered tetracene columns with a tilt angle of 83.8° are the same enantiomer ((*R*)···(*R*) or (*S*)···(*S*)) and are connected by S2···S2′ interactions. Even for the 3-D packing structure formed by self-assembly of the 2-D network sheets of **2**, there is no herringbone packing arrangement (Figures 4a and 5a; see also Figure S4, Supporting Information).[17] The 3-D packing structure of **2** is similar to what is called a γ-motif.[5a,b,10a]

**Table 2. FET Characteristics of Spin-Coated Bis(methylthio)acene-Based Devices Fabricated on Si/$SiO_2$ Substrate[a] and IP Data[b]**

| compd | $\mu_{FET}$ ($cm^2\ V^{-1}\ s^{-1}$) | $V_{th}$ (V) | $I_{on}/I_{off}$ | IP (eV) |
|---|---|---|---|---|
| **1** | $1.3 \times 10^{-2}$ | −5.8 | $>1 \times 10^5$ | 5.3 |
| **2** | $4.0 \times 10^{-2}$ | −1.7 | $>1 \times 10^4$ | 5.8 |
| **3** | NA[c] | | | |

[a] Bottom-contact configuration. [b] ITO/glass substrate. [c] Not available due to no transistor action because of nonuniform films.

In marked contrast to **2**, the regioisomer **3** with a center of symmetry showed a typical herringbone packing arrangement (Figures 3b and 6). There is no S−S interaction between molecules of **3**, wherein the interatomic distance between the two closest sulfur atoms is 4.391 Å. However, there are weak intermolecular S−π interactions, given the interatomic distances of S···C2′ = 3.631 and S···C3′ = 3.422 Å. Thus, the substitution position of two methylthio groups in bis(methylthio)-tetracenes is an important factor in controlling the cofacial π-stacked packing arrangement of the tetracene rings.

**OFET Properties.** The solubility of bis(methylthio)acenes allowed us to study the fabrication of OFETs by a solution process. OFET devices incorporating compounds **1** and **2** with a bottom-contact configuration were fabricated on a n-doped Si/$SiO_2$ substrate and gold−chromium bilayer source/drain electrodes by a simple spin-coating process from a 1,2,4-trichlorobenzene solution of **1** or **2**.[17,21] The data for FET characteristics are summarized in Table 2.[21] Parts a and c of Figure 7 exhibit characteristic p-type FET behavior of the device using **1**. The output characteristics display very good saturation behavior. The


dx.doi.org/10.1021/jo200696a |*J. Org. Chem.* 2011, 76, 5018–5025

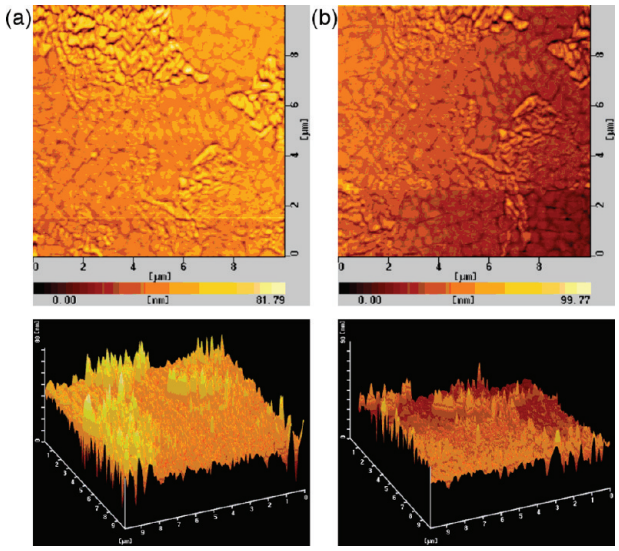


**Figure 8.** AFM images of spin-coated films of (a) **1** and (b) **2** on $SiO_2$.

transfer characteristics show a turn-on voltage of +10 V and a threshold voltage ($V_{th}$) of −5.8 V. The carrier mobility ($\mu_{FET}$) extracted from the saturated regime is as high as $1.3 \times 10^{-2}$ $cm^2$ $V^{-1}$ $s^{-1}$ with a current on/off ratio ($I_{on}/I_{off}$) of over $10^5$. The device using **2** demonstrated $\mu_{FET} = 4.0 \times 10^{-2}$ $cm^2$ $V^{-1}$ $s^{-1}$ with an $I_{on}/I_{off} > 1 \times 10^4$ and $V_{th} = -1.7$ V (Figure 7b,d). It is noted that both of the devices using compounds **1** and **2** exhibit relatively low $V_{th}$ values, even though values of $\mu_{FET}$ and $I_{on}/I_{off}$ are moderate.[1] On the other hand, using **3** as a regioisomer of **2** did not give uniform films, which led to poor coverage and therefore no transistor behavior was observed. Thus, the substitution position of the two methylthio groups in bis(methylthio)tetracenes is also an important factor in device fabrication for OFETs.

Mobilities of spin-coated thin film transistor of **1** and **2** observed here were 1 order of magnitude lower than that of unsubstituted spin-cast pentacene,[22] probably due to roughness of thin films of **1** and **2**. Figure 8 shows the surface morphologies of the spin-coated films of **1** from 1,2,4-trichlorobenzene and **2** from chloroform on $SiO_2$ observed by atomic force microscopy (AFM). Both thin film surfaces are homogeneous but rough, wherein average film thickness (and height of salient region) are ca. 40−45 nm (80 nm) for **1** and 35−40 nm (90 nm) for **2**.

The ionization potential (IP) of spin-coated films of **1** and **2** was measured by photoelectron yield spectroscopy in vacuo (Figure S13, Supporting Information).[17] The IPs of **1** and **2** were determined to be 5.3 and 5.8 eV, respectively (Table 2). This result indicates that the HOMO energy difference between **1** and **2** in spin-coated films is approximately comparable with that based on DFT calculations (Table 1).

## CONCLUSION

We have synthesized 5,12-bis(methylthio)tetracene (**2**) and 5,11-bis(methylthio)tetracene (**3**) and revealed that **2** and **3** lower both HOMO and LUMO energy levels and reduce the HOMO−LUMO gap relative to those of tetracene. We have presented that S−S and S−$\pi$ interactions generally induce cofacial $\pi$-stacking of bis(methylthio)acenes; i.e., 9,10-bis(methylthio)anthracene (**4**),[9a] **2** (this work), and 6,13-bis(methylthio)pentacene (**1**)[10a] self-assemble into 1-D slipped-cofacial $\pi$-stacked acene columns by the assistance of S−S and S−$\pi$ interactions. In contrast, **3** exhibited a herringbone packing arrangement without S−S interactions. We have also demonstrated that **1** and **2** serve as solution-processable semiconductor materials for OFETs. The spin-coated films of **1** and **2**, which are soluble, with a bottom-contact device configuration exhibit field-effect hole mobilities as high as $1.3 \times 10^{-2}$ and $4.0 \times 10^{-2}$ $cm^2$ $V^{-1}$ $s^{-1}$ with current on/off ratios of over $10^5$ and $10^4$, respectively, whereas **3**, which is also soluble, showed no transistor behavior because of nonuniform films. Thus, the substitution position of the two methylthio groups in bis(methylthio)tetracenes is a very important factor in controlling the cofacial $\pi$-stacked packing arrangement of the tetracene ring, as well as in fabricating OFET devices by a solution process.

Studies on the effect of the introduction of multiple methylthio groups in other polycyclic aromatic hydrocarbons to control their crystal packing structures and OFET properties are currently in progress.

## EXPERIMENTAL SECTION

**General Methods.** $CH_2Cl_2$ and $Et_2O$ were distilled from $CaH_2$ and sodium−benzophenone ketyl, respectively, under an argon atmosphere. The other solvents and all commercially available reagents were used without any purification. $^1H$ and $^{13}C$ NMR spectra were recorded at 400 and 100 MHz, respectively.

*trans-5,12-Dihydroxy-5,12-dihydrotetracene (**6**).* To a suspension of 5,12-tetracenequinone (**5**) (7.03 g, 27.2 mmol) in MeOH (350 mL) at 0 °C under Ar was slowly added $NaBH_4$ (4.12 g, 109 mmol). The reaction mixture was stirred at 0 °C for 0.5 h and at room temperature for 2 h and then quenched with $H_2O$ (100 mL) at 0 °C. The resulting mixture was filtered and washed with $H_2O$ and then cold MeOH. The resulting solid was purified by reprecipitation with THF−$CHCl_3$ to give **6** as an off-white solid (4.98 g, 70% yield): mp 184 °C; $^1H$ NMR (DMSO-$d_6$) $\delta$ 8.08 (s, 2H), 7.93 (dd, $J$ = 6.2 and 3.1 Hz, 2H), 7.65 (dd, $J$ = 5.5 and 3.1 Hz, 2H), 7.46 (dd, $J$ = 6.2 and 3.1 Hz, 2H), 7.29 (dd, $J$ = 5.5 and 3.1 Hz, 2H), 6.45 (d, $J$ = 7.1 Hz, 2H), 5.56 (d, $J$ = 7.1 Hz, 2H); $^{13}C$ NMR (DMSO-$d_6$) $\delta$ 139.4, 138.4, 131.7, 127.6, 126.0, 125.5, 122.5, 121.1, 66.7. Anal. Calcd for $C_{18}H_{14}O_2$: C, 82.42; H, 5.38. Found: C, 82.26; H, 5.59.

*trans-5,12-Bis(methylthio)-5,12-dihydrotetracene (**7**).* To a suspension of $CH_3SNa$ (527 mg, 7.52 mmol) in dry $CH_2Cl_2$ (10 mL) at 0 °C under Ar was added acetic acid (430 $\mu$L, 7.51 mmol). This mixture was used as $CH_3SH$ quickly without any purification, which was added by cannula to a heterogeneous mixture of **6** (489 mg, 1.86 mmol) and $ZnI_2$ (1.19 g, 3.72 mmol) in dry $CH_2Cl_2$ (50 mL) at 0 °C under Ar. The resulting mixture was stirred at room temperature for 20 h and then quenched with $H_2O$. The mixture was extracted with $CH_2Cl_2$. The organic layer was washed with $H_2O$ and brine and dried over $Na_2SO_4$. After evaporation of solvents, the residue was purified by column chromatography on silica gel eluted with $CH_2Cl_2$−hexane (1:3 and then 1:2) to give **7** as a white solid (382 mg, 64% yield): mp 134 °C; $^1H$ NMR ($CDCl_3$) $\delta$ 7.85 (dd, $J$ = 6.3 and 3.4 Hz, 2H), 7.84 (s, 2H), 7.49 (dd, $J$ = 6.3 and 3.4 Hz, 2H), 7.45 (dd, $J$ = 5.7 and 3.4 Hz, 2H), 7.33 (dd, $J$ = 5.7 and 3.4 Hz, 2H), 5.18 (s, 2H), 2.31 (s, 6H); $^{13}C$ NMR ($CDCl_3$) $\delta$ 136.7, 134.6, 132.4, 129.1, 127.6, 127.5, 127.4, 126.2, 49.6, 17.6. Anal. Calcd for $C_{20}H_{18}S_2$: C, 74.49; H, 5.63. Found: C, 74.31; H, 5.86.

*5,12-Bis(methylthio)tetracene (**2**).* To a mixture of **7** (323 mg, 1.00 mmol) and tetrachloro-1,4-benzoquinone (493 mg, 2.01 mmol) under Ar was added Ar-saturated $CHCl_3$ (50 mL). The resulting mixture was stirred at 60 °C for 43 h under Ar in the dark. Workup and purification were carried out under air but without room light. After cooling to room temperature and evaporation of $CHCl_3$, the residue was passed through short column of silica gel eluted with $CH_2Cl_2$−hexane (1:20), and the


dx.doi.org/10.1021/jo200696a |J. Org. Chem. 2011, 76, 5018–5025

deep red band was collected. After evaporation of solvents, the residue was purified by reprecipitation with $CH_2Cl_2$−MeOH to give **2** as a red solid (203 mg, 63% yield): mp 184 °C; $^1$H NMR ($CDCl_3$) $\delta$ 9.72 (s, 2H), 9.07 (dd, $J$ = 6.8 and 3.4 Hz, 2H), 8.15 (dd, $J$ = 6.8 and 3.4 Hz, 2H), 7.58 (dd, $J$ = 6.8 and 3.4 Hz, 2H), 7.49 (dd, $J$ = 6.8 and 3.4 Hz, 2H), 2.50 (s, 6H); $^{13}$C NMR ($CDCl_3$) $\delta$ 134.1, 133.8, 132.1, 132.0, 128.6, 127.8, 126.7, 126.4, 125.9, 20.4. Anal. Calcd for $C_{20}H_{16}S_2$: C, 74.96; H, 5.03. Found: C, 75.01; H, 5.17.

*5,11-Bis(methylthio)tetracene* (**3**). A 1:1 mixture of 5,11- and 5,12-dibromotetracenes (**8** and **8′**) (1.78 g), which was prepared in 82% yield according to the literatures,[14b,15c] was recrystallized from hot toluene to give a 2.55:1 mixture of them (1.15 g, 2.98 mmol in total). To this mixture in dry $Et_2O$ (500 mL) at −78 °C under Ar in the dark was added a *n*-pentane solution of *t*-BuLi (1.58 M, 8.3 mL, 13.1 mmol), and the resulting mixture was stirred at −78 °C for 1 h, and then dimethyl disulfide (2.1 mL, 23.3 mmol) was added to this mixture at −78 °C. The reaction mixture was allowed to warm to room temperature overnight. Workup and purification were carried out under air but without room light. The resulting reaction mixture was quenched with $H_2O$ at 0 °C and then extracted with $Et_2O$. The organic layer was washed with $H_2O$ and brine and dried over $Na_2SO_4$. After evaporation of solvent, the residue was subjected to column chromatography on silica gel eluted with $CHCl_3$−hexane (1:1) to give a 3.00:1 mixture of **3** and **2** (316 mg in total, corresponding to 35% yield for **3** and 29% yield for **2**). This mixture of **3** and **2** was recrystallized from hot toluene (twice) and then from hot $CHCl_3$−hexane (twice) to give analytical pure **3** as a red solid (140 mg): mp 256 °C; $^1$H NMR ($CDCl_3$) $\delta$ 9.74 (s, 2H), 8.95 (d, $J$ = 9.0 Hz, 2H), 8.16 (d, $J$ = 8.5 Hz, 2H), 7.59 (dd, $J$ = 9.0 and 6.6 Hz, 2H), 7.50 (dd, $J$ = 8.5 and 6.6 Hz, 2H), 2.49 (s, 6H); $^{13}$C NMR ($CDCl_3$) $\delta$ 134.1, 132.4, 132.2, 132.0, 130.0, 128.2, 127.0, 126.8, 125.4, 20.4. Anal. Calcd for $C_{20}H_{16}S_2$: C, 74.96; H, 5.03. Found: C, 74.87; H, 5.22.

**X-ray Data Collection and Crystal Structure Determination of 2 and 3.** The data were measured using a CCD area detector, using Mo−Kα graphite monochromated radiation ($\lambda$ = 0.71073 Å). The structure was solved by direct methods using the program SHELXS-97.[23] The refinement and all further calculations were carried out using SHELXL-97.[23] The H-atoms were included in calculated positions and treated as riding atoms using the SHELXL default parameters. The non-H atoms were refined anisotropically, using weighted full-matrix least-squares on $F^2$. Crystal data and structure refinement are listed in Tables S1 and S2 (Supporting Information).[17] The X-ray experimental details are described in the form of a CIF.[17]

## ■ ASSOCIATED CONTENT

**Supporting Information.** Additional data and X-ray crystallographic data (CIF). This material is available free of charge via the Internet at http://pubs.acs.org.

## ■ AUTHOR INFORMATION

**Corresponding Author**
*E-mail: skkobay@ipc.shizuoka.ac.jp.

## ■ ACKNOWLEDGMENT

This work was supported in part by PRESTO, JST, and the Asahi Glass Foundation. We thank Dr. Kengo Suzuki (Hamamatsu Photonics K.K.) and Mr. Yutaka Fujiwara (Shizuoka University) for measurements of fluorescence quantum yields and lifetimes of **1**−**3**.

## ■ REFERENCES

(1) (a) Anthony, J. E. *Chem. Rev.* **2006**, *106*, 5028–5048. (b) Würthner, F.; Schmidt, R. *ChemPhysChem* **2006**, *7*, 793–797. (c) Murphy, A. R.; Fréchet, J. M. J. *Chem. Rev.* **2007**, *107*, 1066–1096. (d) Anthony, J. E. *Angew. Chem., Int. Ed.* **2008**, *47*, 452–483. (e) Allard, S.; Forster, M.; Souharce, B.; Thiem, H.; Scherf, U. *Angew. Chem., Int. Ed.* **2008**, *47*, 4070–4098.

(2) Jurchescu, O. D.; Baas, J.; Palstra, T. T. M. *Appl. Phys. Lett.* **2004**, *84*, 3061–3063.

(3) (a) Sundar., V. C.; Zaumseil, J.; Podzorov, V.; Menard, E.; Willet, R. L.; Someya, T.; Gershenson, M. E.; Rogers, J. A. *Science* **2004**, *303*, 1644–1646. (b) Takeya, J.; Yamagishi, M.; Tominari, Y.; Hirahara, R.; Nakazawa, Y.; Nishikawa, T.; Kawase, T.; Shimoda, T.; Ogawa, S. *Appl. Phys. Lett.* **2007**, *90*, 102120–1−3.

(4) Klauk, H.; Halik, M.; Zschieschang, U.; Schmid, G.; Radlik, W.; Weber, W. *J. Appl. Phys.* **2002**, *92*, 5259–5263.

(5) (a) Desiraju, G. R.; Gavezzotti, A. *Acta Crystallogr. Sect. B* **1989**, *45*, 473–482.(b) Desiraju, G. R. *Crystal Engineering: The Design of Organic Solids*; Elsevier: Amsterdam, 1989; Chapter 4. (c) Cornil, J.; Calbert, J. P.; Brédas, J. L. *J. Am. Chem. Soc.* **2001**, *123*, 1250–1251. (d) Fritz, S. E.; Martin, S. M.; Frisbie, C. D.; Ward, M. D.; Toney, M. F. *J. Am. Chem. Soc.* **2004**, *126*, 4084–4085.

(6) (a) Brédas, J.-L.; Calbert, J. P.; da Silva Filho, D. A.; Cornil., J. *Proc. Natl. Acad. Sci. U.S.A.* **2002**, *99*, 5804–5809. (b) Haddon, R. C.; Chi, X.; Itkis, M. E.; Anthony, J. E.; Eaton, D. L.; Siegrist, T.; Mattheus, C. C.; Palstra, T. T. M. *J. Phys. Chem. B* **2002**, *106*, 8288–8292. (c) Curtis, M. D.; Cao, J.; Kampf, J. W. *J. Am. Chem. Soc.* **2004**, *126*, 4318–4328. (d) Brédas, J.-L.; Beljonne, D.; Coropceanu, V.; Cornil, J. *Chem. Rev.* **2004**, *104*, 4971–5003. (e) Deng, W.-Q.; Goddard, W. A., III. *J. Phys. Chem. B* **2004**, *108*, 8614–8621. (f) da Silva Filho, D. A.; Kim, E.-G.; Brédas, J.-L. *Adv. Mater.* **2005**, *17*, 1072–1076.

(7) Silvestri, F.; Marrocchi, A.; Seri, M.; Kim, C.; Marks, T. J.; Facchetti, A.; Taticchi, A. *J. Am. Chem. Soc.* **2010**, *132*, 6108–6123.

(8) (a) Anthony, J. E.; Brooks, J. S.; Eaton, D. L.; Parkin, S. R. *J. Am. Chem. Soc.* **2001**, *123*, 9482–9483. (b) Anthony, J. E.; Eaton, D. L.; Parkin, S. R. *Org. Lett.* **2002**, *4*, 15–18. (c) Payne, M. M.; Parkin, S. R.; Anthony, J. E.; Kuo, C.-C.; Jackson, T. N. *J. Am. Chem. Soc.* **2005**, *127*, 4986–4987. (d) Subramanian, S.; Park, S. K.; Parkin, S. R.; Podzorov, V.; Jackson, T. N.; Anthony, J. E. *J. Am. Chem. Soc.* **2008**, *130*, 2706–2707.

(9) (a) Kobayashi, K.; Masu, H.; Shuto, A.; Yamaguchi, K. *Chem. Mater.* **2005**, *17*, 6666–6673. (b) Sasaki, H.; Wakayama, Y.; Chikyow, T.; Barrena, E.; Dosch, H.; Kobayashi, K. *Appl. Phys. Lett.* **2006**, *88*, 081907–1−3.

(10) (a) Kobayashi, K.; Shimaoka, R.; Kawahata, M.; Yamanaka, M.; Yamaguchi, K. *Org. Lett.* **2006**, *8*, 2385–2388. (b) Wakayama, Y.; Hayakawa, R.; Chikyow, T.; Machida, S.; Nakayama, T.; Egger, S.; de Oteyza, D. G.; Dosch, H.; Kobayashi, K. *Nano Lett.* **2008**, *8*, 3273–3277.

(11) For S−S interactions for molecular ordering, see also: (a) Werz, D. B.; Gleiter, R.; Rominger, F. *J. Am. Chem. Soc.* **2002**, *124*, 10638–10639. (b) Gleiter, R.; Werz, D. B. *Chem. Lett.* **2005**, *34*, 126–131. (c) Bleiholder, C.; Werz, D. B.; Köppel, H.; Gleiter, R. *J. Am. Chem. Soc.* **2006**, *128*, 2666–2674.

(12) (a) Kaur, I.; Jia, W.; Kopreski, R. P.; Selvarasah, S.; Dokmeci, M. R.; Pramanik, C.; McGruer, N. E.; Miller, G. P. *J. Am. Chem. Soc.* **2008**, *130*, 16274–16286. (b) Kaur, I.; Stein, N. N.; Kopreski, R. P.; Miller, G. P. *J. Am. Chem. Soc.* **2009**, *131*, 3424–3425. (c) Kaur, I.; Jazdzyk, M.; Stein, N. N.; Prusevich, P.; Miller, G. P. *J. Am. Chem. Soc.* **2010**, *132*, 1261–1263.

(13) For selected examples of sulfur-containing heretoacenes, see ref 8c,8d and: (a) Laquindanum, J. G.; Katz, H. E.; Lovinger, A. J. *J. Am. Chem. Soc.* **1998**, *120*, 664–672. (b) Li, X.-C.; Sirringhaus, H.; Garnier, F.; Holmes, A. B.; Moratti, S. C.; Feeder, N.; Clegg, W.; Teat, S. J.; Friend, R. H. *J. Am. Chem. Soc.* **1998**, *120*, 2206–2207. (c) Mas-Torrent, M.; Durkut, M.; Hadley, P.; Ribas, X.; Rovira, C. *J. Am. Chem. Soc.* **2004**, *126*, 984–985. (d) Takimiya, K.; Kunugi, Y.; Konda, Y.; Niihara, N.; Otsubo, T. *J. Am. Chem. Soc.* **2004**, *126*, 5084–5085. (e) Meng, H.; Sun, F.; Goldfinger, M. B.; Jaycox, G. D.; Li, Z.; Marshall, W. J.; Blackman, G. S. *J. Am. Chem. Soc.* **2005**, *127*, 2406–2407. (f) Xiao, K.; Liu, Y.; Qi, T.;

Zhang, W.; Wang, F.; Gao, J.; Qiu, W.; Ma, Y.; Cui, G.; Chen, S.; Zhan, X.; Yu, G.; Qin, J.; Hu, W.; Zhu, D. *J. Am. Chem. Soc.* **2005**, *127*, 13281–13286. (g) Naraso; Nishida, J.; Kumaki, D.; Tokito, S.; Yamashita, Y. *J. Am. Chem. Soc.* **2006**, *128*, 9598–9599. (h) Takimiya, K.; Ebata, H.; Sakamoto, K.; Izawa, T.; Otsubo, T.; Kunugi, Y. *J. Am. Chem. Soc.* **2006**, *128*, 12604–12605. (i) Briseno, A.; Miao, Q.; Ling, M.-M.; Reese, C.; Meng, H.; Bao, Z.; Wudl, F. *J. Am. Chem. Soc.* **2006**, *128*, 15576–15577. (j) Tang, M. L.; Okamoto, T.; Bao, Z. *J. Am. Chem. Soc.* **2006**, *128*, 16002–16003. (k) Yamamoto, T.; Takimiya, K. *J. Am. Chem. Soc.* **2007**, *129*, 2224–2225. (l) Yamada, K.; Okamoto, T.; Kudoh, K.; Wakamiya, A.; Yamaguchi, S.; Takeya, J. *Appl. Phys. Lett.* **2007**, *90*, 072102−1–3. (m) Tang, M. L.; Reichardt, A. D.; Miyaki, N.; Stoltenberg, R. M.; Bao, Z. *J. Am. Chem. Soc.* **2008**, *130*, 6064–6065. (n) Didane, Y.; Mehl, G. H.; Kumagai, A.; Yoshimoto, N.; Videlot-Ackermann, C.; Brisset, H. *J. Am. Chem. Soc.* **2008**, *130*, 17681–17683.

(14) For selected examples of OFET properties of functionalized tetracenes, see ref 3 and: (a) Tulevski, G. S.; Miao, Q.; Fukuto, M.; Abram, R.; Ocko, B.; Pindak, R.; Steigerwald, M. L.; Kagan, C. R.; Nuckolls, C. *J. Am. Chem. Soc.* **2004**, *126*, 15048–15050. (b) Moon, H.; Zeis, R.; Borkent, E.-J.; Besnard, C.; Lovinger, A. J.; Siegrist, T.; Kloc, C.; Bao, Z. *J. Am. Chem. Soc.* **2004**, *126*, 15322–15323. (c) Merlo, J. A.; Newman, C. R.; Gerlach, C. P.; Kelley, T. W.; Muyres, D. V.; Fritz, S. E.; Toney, M. F.; Frisbie, C. D. *J. Am. Chem. Soc.* **2005**, *127*, 3997–4009. (d) Schmidt, R.; Göttling, S.; Leusser, D.; Stalke, D.; Krause, A.-M.; Würthner, F. *J. Mater. Chem.* **2006**, *16*, 3708–3714. (e) Paraskar, A. S.; Reddy, A. R.; Patra, A.; Wijsboom, Y. H.; Gidron, O.; Shimon, L. J. W.; Leitus, G.; Bendikov, M. *Chem.—Eur. J.* **2008**, *14*, 10639–10647. (f) Kimoto, T.; Tanaka, K.; Sakai, Y.; Ohno, A.; Yoza, K.; Kobayashi, K. *Org. Lett.* **2009**, *11*, 3658–3661.

(15) For selected examples of other functionalized tetracenes, see: (a) Odom, S. A.; Parkin, S. R.; Anthony, J. E. *Org. Lett.* **2003**, *5*, 4245–4248. (b) Del Guerzo, A.; Olive, A. G. L.; Reichwagen, J.; Hopf, H.; Desvergne, J.-P. *J. Am. Chem. Soc.* **2005**, *127*, 17984–17985. (c) Kyushin, S.; Ishikita, Y.; Matsumoto, H.; Horiuchi, H.; Hiratsuka, H. *Chem. Lett.* **2006**, *35*, 64–65. (d) Chen, Z.; Muller, P.; Swager, T. M. *Org. Lett.* **2006**, *8*, 273–276. (e) Liang, Z.; Zhao, W.; Wang, S.; Tang, Q.; Lam, S.-C.; Miao, Q. *Org. Lett.* **2008**, *10*, 2007–2010. (f) Kitamura, C.; Abe, Y.; Ohara, T.; Yoneda, A.; Kawase, T.; Kobayashi, T.; Naito, H.; Komatsu, T. *Chem.—Eur. J.* **2010**, *16*, 890–898.

(16) Guindon, Y.; Frenette, R.; Fortin, R.; Rokach, J. *J. Org. Chem.* **1983**, *48*, 1357–1359.

(17) See the Supporting Information.

(18) The fluorescence spectra, fluorescence quantum yields, and fluorescence lifetimes of **1**, **2**, **3**, and tetracene were measured in Ar-saturated $CH_2Cl_2$ (Figure S9 and Table S3, Supporting Information).[17] The fluorescence quantum yields and lifetimes of them were significantly low and short, respectively. In particular, the fluorescence quantum yield of **1** ($\Phi_f$ = < 0.001, below measurable limits) was much lower than those of **2** ($\Phi_f$ = 0.028) and **3** ($\Phi_f$ = 0.127), and the fluorescence lifetime of **1** ($\tau_s$ = < 0.15 ns, below measurable limits) was much shorter than those of **2** ($\tau_s$ = 0.97 ns) and **3** ($\tau_s$ = 3.69 ns). Thus, one reason why **1** is more resistant to photooxidation than **2** and **3** may be a consequence of a shorter excited state lifetime of **1** relative to those of **2** and **3**.

(19) The sum of van der Waals radii of two atoms is as follows: S···S = $3.60^a$ $(3.70)^b$ Å; S···C = $3.50^a$ $(3.55)^b$ Å.(a) Elemental Radii in the Cambridge Structural Database, Cambridge Crystallographic Data Centre, Cambridge. (b) Pauling, L. *The Nature of the Chemical Bond*, 3rd ed.; Cornell University Press: Ithaca, NY, 1973.

(20) Maitland, G. C.; Rigby, M.; Smith, E. B.; Wakeham, W. A. *Intermolecular Forces*; Clarendon Press: Oxford, 1981.

(21) The TFT devices were fabricated in yellow light and were measured in the dark. The devices measured two structures (bottom electrode contact and top electrode contact). These values were the average of more than three samples.

(22) Minakata, T.; Natsume, Y. *Synth. Met.* **2005**, *153*, 1–4.

(23) Sheldrick, G. M. *SHELXS-97 and SHELXL-97*, University of Göttingen, Göttingen, Germany, 1997.